

CONF-860605--7

Symposium on the Effects of Radiation on Materials

Measurements of $^{10}\text{B}(n,\text{He})$ Reaction Rates
in a Mockup Control Rod in ZPPR

S. B. Brumbach and P. J. Collins

CONF-860605--7

Argonne National Laboratory
Idaho Falls, Idaho 83403

DE86 007518

and

B. M. Oliver
Rockwell International
Canoga Park, California 91304

The submitted manuscript has been authored by a contractor of the U. S. Government under contract No. W-31-109-ENG-38. Accordingly, the U. S. Government retains a nonexclusive, royalty-free license to publish or reproduce the published form of this contribution, or allow others to do so, for U. S. Government purposes.

DISCLAIMER**MASTER**

This report was prepared as an account of work sponsored by an agency of the United States Government. Neither the United States Government nor any agency thereof, nor any of their employees, makes any warranty, express or implied, or assumes any legal liability or responsibility for the accuracy, completeness, or usefulness of any information, apparatus, product, or process disclosed, or represents that its use would not infringe privately owned rights. Reference herein to any specific commercial product, process, or service by trade name, trademark, manufacturer, or otherwise does not necessarily constitute or imply its endorsement, recommendation, or favoring by the United States Government or any agency thereof. The views and opinions of authors expressed herein do not necessarily state or reflect those of the United States Government or any agency thereof.

Work supported by the U.S. Department of Energy, "Nuclear Energy Programs under Contract W-31-109-Eng-38.

JMF

Measurements of $^{10}\text{B}(n,\text{He})$ Reaction Rates
in a Mockup Control Rod in ZPPR

S. B. Brumbach and P. J. Collins

Argonne National Laboratory
Idaho Falls, Idaho 83403

and

B. M. Oliver
Rockwell International
Canoga Park, California 91304

Introduction

Knowledge of the $^{10}\text{B}(n,\text{He})$ reaction rate in a control rod in a fast neutron spectrum is important in control rod design studies for fast reactors. Production of helium (and also lithium) in the neutron absorption reactions in ^{10}B results in control rod swelling, buildup of gas pressure and a reduction in thermal conductivity which can limit the lifetime of the control rod. Methods for calculating the $^{10}\text{B}(n,\text{He})$ rates in control rods have been discussed by Rowlands, et al.¹ and by McFarlane and Collins.² The calculation of $^{10}\text{B}(n,\text{He})$ rates near the tip of a control rod is particularly challenging because of steep gradients in the capture rate between the surface and the interior of the rods. Alpha and gamma heating of the surface pellets can be severe relative to the rod average.

Given the difficulty in calculating neutron capture rates in control rods, a measurement technique to provide reaction rate values is of interest. Previous measurements of reaction rates in control rods have been sparse. One technique which has been used is calorimetry which measures only the heat produced in a sample of control-rod material. A second technique utilized foils of metallic uranium (normally ^{235}U) placed between pellets of absorber material in a mockup

control rod irradiated in a critical assembly. Measured ^{235}U fission rates can be used to estimate ^{10}B capture rates using calculated values for the reaction rate ratio. Foil irradiation results have been reported by Broomfield, et al.³

This paper reports the first direct measurement of ^{10}B capture rate in a mockup control rod in a critical assembly. The experiment used the helium accumulation fluence monitor (HAFM) technique. The HAFM technique has been used by Farrar, Oliver and co-workers⁴⁻⁶ to measure the $^{10}\text{B}(n,\text{He})$ reaction rates in a variety of fast neutron spectra. In the HAFM technique, ^{10}B in a small, sealed, stainless steel capsule is irradiated producing helium. Following irradiation, the capsule and contents are vaporized in a vacuum system and the amount of helium released is measured by isotope-dilution mass spectrometry. The applicability of the HAFM technique in the Zero Power Plutonium Reactor (ZPPR) has been demonstrated in the fuel regions of the ZPPR-13C assembly.⁷⁻⁸ Following this successful demonstration, an irradiation of ^{10}B -containing HAFMs was conducted in a mockup pin-type control rod in the ZPPR-12 Metal Blanket assembly. This ZPPR-12MB irradiation was intended as a demonstration of the HAFM method in a B₄C control assembly, with more detailed measurements in a larger, more prototypic control assembly, planned for the future.

Foils of ^{235}U were also placed between pellets of the control rod in pins symmetrically equivalent to pins containing HAFMs, and, following irradiation their fission rates were measured. The purpose of the foil measurements was to compare the foil and HAFM techniques for their ability to verify calculated ^{10}B capture rates. Lithium-fluoride-

containing HAFMs have been used along with ^{10}B HAFMs in previous experiments ⁴⁻⁷ and served here as a check on the boron measurements.

Experiment Description

The ZPPR-12MB Assembly

The ZPPR critical assembly is a split-table device and each half contains an array of square cross section tubes. Each tube can accommodate a drawer which contains plates of fissile, fertile, coolant and structural material enabling construction of a full-size replica of a fast reactor. The ZPPR-12MB assembly was rather small with a core volume of 352 liters. The composition was typical of a liquid metal-fast breeder reactor (LMFBR) with mixed plutonium-uranium oxide fuel. Because of its small size, the ZPPR-12MB core had a relatively high fissile enrichment and consequently had a neutron spectrum somewhat harder than a typical LMFBR. The two halves of the assembly were reflected about the interface. The loading pattern is shown in Fig. 1. Each square in Fig. 1 represents one matrix tube, about 55 mm square. There were 125 fuel drawers in each assembly half and the total core height was 914 mm. Sodium coolant and fuel were sealed in stainless steel cans. The fuel was in the form of a Pu-U-Mo alloy. Outside the core were radial and axial blankets of depleted uranium metal and reflectors of stainless steel.

Mockup Control Rod

For the $^{10}\text{B}(n,\text{He})$ reaction rate measurements, the central fuel drawer in one assembly half was removed and a mockup control rod assembly was inserted. The control rod consisted of a stack of three

stainless steel calandria, each 304.8 mm long and 51.7 mm square containing sixteen tubes in a square array. A calandria (containing solid steel rods) is shown in Fig. 2. In the ZPPR-12MB experiments, each tube contained a stack of B_4C pellets with the boron enriched to 92% ^{10}B . Each pellet was 25.4 mm long and 9.52 mm in diameter. The calandria closest to the axial center of the assembly did not contain sodium and did not have the normal stainless-steel jacket. The two calandria away from the axial center were filled with sodium and had stainless-steel jackets. The drawer opposite the calandria was a standard fuel drawer rather than a sodium-filled channel that one might expect opposite a half-inserted control rod. This control rod mockup does not reproduce in detail the geometry expected in a power-reactor control assembly, but it does provide some of the neutronic environments encountered in conventional control assemblies and does provide an appropriate configuration for testing the ability of the HAFM technique to provide $^{10}B(n,He)$ reaction rate values.

To compensate for the reactivity lost when removing fuel and adding boron, blanket drawers at the core/blanket boundary were converted to fuel drawers.

HAFM Capsules and Foils

The HAFM capsules were manufactured at Rockwell from thin-walled (0.076 mm), 2.36 mm-OD, type 304 stainless-steel tubing. A type 303 stainless-steel plug, 1.45 mm long, was electron beam welded on one end. After filling with measured masses of either ^{10}B or 6LiF , a second end plug was welded in place, sealing the capsule. Capsule lengths were about 12.4 mm. Sample masses were about 37 mg for the ^{10}B and about 43 mg for the 6LiF . The ^{10}B enrichment was 93.10% and the 6Li enrichment was 99.10%.

The uranium foils contained about 93% ^{235}U , were 0.13 mm thick and about 8.8 mm in diameter. The ^{235}U mass was typically 115 mg. The foils were covered with 0.0025 mm-thick aluminum discs to prevent fission product loss.

To accommodate the HAFMs, the B₄C pellets were bored with 2.54 mm diameter holes. The holes were oriented either axially along the centerline of the pellet (12.7 mm deep) or radially through the 9.5 mm diameter of the pellet, 6.4 mm from one face of the pellet. The holes were made using a spark erosion technique.

Because the inside diameter of a calandria tube is 9.87 mm and the HAFM is about 12.4 mm long, a radially oriented HAFM required holes to be cut in the wall of the calandria tube. To insert the HAFM through the calandria tube and pellet, it was necessary to use a calandria which did not contain sodium and which had its outer stainless steel jacket removed. Also, only exterior tubes on the outer calandria edge were practical for placing radially oriented HAFMs.

A cross-sectional view of a pin calandria showing the pin numbering scheme is given in Fig. 3. There are three different pin environments; corner pins (1, 4, 13 and 16), edge pins (2, 3, 8, 12, 15, 14, 9 and 5) and interior pins (6, 7, 10 and 11). Axially oriented HAFMs were irradiated in each of the three environments. Radially oriented HAFMs were in pin 9 which had an environment equivalent to pin 5.

Empty HAFMs, serving as blanks, were irradiated near the tip of the rod in pins 1 and 15. Lithium fluoride-containing HAFMs were irradiated in the first two pellets in pin 8 and in the first three pellets in pin 4.

Foils could only be irradiated between pellets or at the very front of the calandria. Foils were placed in pins with environments equivalent to the pins containing HAFMs and with axial locations as close as possible to the axial locations of the HAFMs.

Larger foils of ^{235}U , 12.5 mm in diameter and mounted in stainless steel holders, were irradiated in fuel drawers along the x and y axes of the assembly to provide flux shape information and to provide a normalization for rates measured in the control rod. Typical masses for these foils was 230 mg.

The HAFMs and foils were irradiated for about 2000 watt hours.

Helium Analysis and Results

Following irradiation, the nineteen boron, lithium and empty HAFMs were returned to Rockwell and were analysed for their helium content. Analysis was by isotope-dilution mass spectrometry.⁴ Each analysis involved vaporizing the complete capsule and its contents in a resistance-heated graphite crucible in one of the mass spectrometer system's high-temperature vacuum furnaces. The absolute amount of ^4He released was then determined from a measurement of the $^4\text{He}/^3\text{He}$ ratio in which the amount of ^3He "spike", about 2×10^{13} atoms, was accurately known.

The ^3He spikes used for the ratio measurements were obtained by expanding and partitioning a known quantity of ^3He gas through a succession of calibrated volumes.⁴ The mass spectrometer was repeatedly calibrated for mass sensitivity during each series of measurements by analyzing known mixtures of ^3He and ^4He . Small amounts of ^3He ($\sim 5 \times 10^9$ atoms) in the ^6LiF HAFMs, resulting from the decay of generated tritium, were accounted for in the analysis.

Table 1 gives the measured helium production in the irradiated ^{10}B and ^6LiF HAFMs from ZPPR-12MB. The total number of helium atoms produced was about 1×10^{12} for the ^{10}B and 0.3×10^{12} for the lithium. The atom fractions were about 0.4×10^{-9} for ^{10}B and 0.3×10^{-9} for ^6Li . The helium production rates are in reactions per atom per second normalized to a reactor power of approximately 1 watt as measured by an ex-core power monitor. Measured helium in the two empty HAFMs was zero within measurement uncertainties.

The helium measurements were corrected for background helium released during the vaporization process by the graphite crucibles and vacuum furnace. This background correction averaged about 6×10^9 atoms. The ^6LiF helium reaction rates were also corrected for helium generation from $^{19}\text{F}(n,\text{He})$ reactions. This correction was calculated to be about 0.2% based on numerous earlier HAFM measurements,

Uncertainties in the helium measurements presented in Table 1 are about 0.8% for the ^{10}B HAFMs and about 1.8% for the ^6LiF HAFMs. These uncertainties come largely from two sources: (1) random and systematic uncertainties in the mass spectrometer analysis system, and (2) random uncertainty in the background helium originating from the vacuum furnaces and graphite crucibles used to vaporize each HAFM capsule. Extensive analysis of the mass spectrometer system⁸ has indicated a systematic uncertainty of about 0.3% and a random uncertainty of about 0.5%. An estimate of the random uncertainty associated with the helium release from the vacuum furnace and graphite crucibles was obtained from the helium data from numerous empty crucibles analyzed along with the HAFMs during the present series of measurements. Analysis of these

empty-crucible data indicated an uncertainty of about 5×10^9 atoms. Combining the various uncertainties in quadrature gives the estimated total uncertainty of 0.8% for the ^{10}B HAFMs and 1.8% for the ^6LiF HAFMs.

The results in Table 1 show, as expected, a decrease in the ^{10}B and ^6Li reaction rates with increasing axial depth into the control rod pins. This decrease is about 18% in all pins for the 63.4 mm change in depth (distance between HAFM centers). Also, at all axial depths, rates are highest in the corner pin, lowest in the interior pin and intermediate in the edge pins. The variation in boron capture within a plane of the control rod is 10% to 12% at all three axial depths. Relative reaction rates, based on unity for the highest value (pin 13, pellet 1 for ^{10}B , pin 4, pellet 1 for ^6Li) are shown in Fig. 4. The ^{10}B and ^6Li rates are normalized separately.

It should be noted that the measured (n,He) reaction rates are all spatial averages over the effective length of the HAFM. The ^{10}B -filled length of the HAFMs is about 9.5 mm, so the ^{10}B just spans the pellet diameter in the radially oriented HAFMs. Because the measured values are spatial averages, the 9.5 mm sample length limits the spatial resolution of the measurement.

Foil Counting and Results

The absolute number of fissions which occurred in the ^{235}U foils was determined by counting gamma rays from fission products in a calibrated Ge(Li) counting system. The counting system and the calibration procedures are described elsewhere.^{9,10,11} Typical uncertainties in relative fission rate values are 0.6%, while uncertainties in absolute values are about 1.5%. Measured ^{235}U fission rates are given in Table 2 for the foils irradiated in the mockup

control rod. The units are the number of fissions per atom of ^{235}U per second normalized to a reactor power of approximately one watt.

As was the case for the HAFMs, the $^{235}\text{U}(n,f)$ rates decrease with increasing depth into the control rod and rates are highest in the corner pin, lowest in the interior pin and intermediate in the edge pin. There appears to be a larger variation in the fission rate in the interior pin than in the corner pin with the edge pin again intermediate. Results for the foils at the outer surfaces of the pins are difficult to interpret because they do not sample the flux or spectrum within the pin.

Calculated $^{235}\text{U}(n,f)$, $^{10}\text{B}(n,\text{He})$ and $^6\text{Li}(n,\text{He})$ Reaction Rates

Reaction rate values were calculated for $^{235}\text{U}(n,f)$, $^{10}\text{B}(n,\text{He})$ and $^6\text{Li}(n,\text{He})$ at the foil and HAFM locations in ZPPR-12MB. The calculations used the ANL system of reactor codes. Cross sections were obtained from the ENDF/B-IV general-purpose file. Calculated helium generation in the ^{10}B and ^6Li was limited to the dominant nonthreshold reactions $^{10}\text{B}(n,\alpha)^7\text{Li}$ and $^6\text{Li}(n,\alpha)^3\text{H}$ or $^6\text{Li}(n,\alpha)^3\text{H}$. Helium generation from threshold reactions in either ^{10}B or ^6Li , e.g., $^{10}\text{B}(n,2\alpha)^3\text{H}$ or $^6\text{Li}(n,n'\alpha)^2\text{H}$, is expected to be small (<0.2%), and thus was neglected.

Homogenized cross sections in 28 energy groups for the various ZPPR drawers were produced by the codes MC²-2 and SDX.¹³ The atom densities for each drawer type were obtained from the known average masses of the materials contained in those drawers and from the known drawer volume. The reaction rates were calculated in three-dimensional (x,y,z) geometry with the nodal transport version of the code DIF3D.¹³ One-fourth xy plane symmetry was assumed with full z-dimensional modelling to accommodate the half-inserted control rod. There was one node per

drawer in the xy plane. In the z dimension, the node spacing was 100 mm for the first 300 mm in each half, and then 150 mm for the remaining 150 mm of core and 450 mm of axial blanket. The control rod cross sections assumed a uniform mix of all isotopes in the node.

Calculated reaction rate values at a specific HAFM or foil location are obtained by polynomial interpolation, consistent with the nodal solution. Values are determined assuming all material is at the center of the HAFM. Calculated reaction rates were not integrated over the dimensions of the HAFMs or foils.

All calculated reaction rates are normalized to provide an average value of unity for the ratio of the calculated (C) to measured (E) ^{235}U fission rates for the 16 measurements of $^{235}\text{U}(n,f)$ in the fuel zone. This normalization procedure is used because relative reaction rates (profiles) and reaction rate ratios are normally of interest. Also, it is difficult to measure absolute power in ZPPR to better than about 5%. The measured $^{235}\text{U}(n,f)$ values and the corresponding C/E values for the measurements in the fuel region are given in Table 3. The standard deviation in C/E for the 16 fission rates is 0.73%. This is only a little larger than the uncertainty in the measured values (0.6%). The C/E values increase monotonically with increasing radius with values about 1% above average at the core edge and about 1% below average near the core center. This variation is similar to that found in the core without any control rod.

Comparison of Measured and Calculated Reaction Rates

The values for the C/E ratio for $^{10}\text{B}(n,\text{He})$ and $^6\text{Li}(n,\text{He})$ measured in the mockup control rod are presented in Table 1. The C/E values for boron are also shown in Fig. 4. For the axially oriented HAFMs, there

is no clear trend in C/E value with axial displacement from the assembly center, and there is also no clear trend in C/E value for the corner, edge or interior pin environments. For the equivalent environments in pin 5 and 9, the difference between average C/E values for the axially and radially oriented HAFMs is about 1.8%.

The relative boron capture rates within the various pins, based on unity for the HAFM closest to the rod tip, are shown in Table 4 for both the measurement and the calculation. The axial profiles of the capture rates are predicted within 2% except for the deepest HAFM in pin 10 where there is a 4% difference.

For ${}^6\text{Li}$, the C/E values are consistent within pins 4 and 8 but are about 5% different between pins. The C/E difference between pins 4 and 8 is not understood.

The C/E values for ${}^{235}\text{U}(n,f)$ rates in the mockup control rod are presented in Table 2. It is clear that there is a problem with the foils at the pin surface compared to the foils in the interior of the pin. As already mentioned, the surface foil environment is difficult to model in a calculation, in part because of the streaming path caused by the small gap at the assembly interface. If the foils at the pin surfaces are ignored, the C/E values within each pin are the same within uncertainties. For the interior pin (number 11), the foil C/E values are 2% to 3% higher than for the other two pins. The relative fission rates within the various pins, based on unity for the foils between the first and second pellets (25.4 mm from the rod tip) are shown in Table 5. The calculation predicts an axial decrease of about 8% going from 25.4 mm to 76.2 mm from the rod tip, which is in good agreement with the measured profiles.

Discussion

The HAFM measurements in ZPPR-12MB demonstrated the usefulness of the technique for obtaining boron capture measurements within B₄C pellets of a control rod. While the ZPPR-12MB control rod mockup was not a realistic model of a power reactor control assembly, the neutronic environments expected in a control assembly were represented. The measured boron capture rates showed the expected trends of decreasing rate with increasing axial depth in the rod and decreasing rates going from exterior to interior pins.

There was a difference of about 2% in capture rates in equivalent pins using axially oriented and radially oriented HAFMs. The HAFM midpoints were equally displaced from the rod tip in both orientations. Given the estimated measurement uncertainty of about 1% for relative capture rates, there appears to be little difference between measurements which integrate reaction rates radially and axially, at least for the geometry and spectrum of ZPPR-12MB.

The boron capture rates calculated using three-dimensional nodal transport methods gave C/E ratios which were consistent within 2% at all locations in the control rod indicating that there was good agreement between calculation and measurement for the relative reaction rates (profiles) within the rod.

Fission rates in ²³⁵U were measured and calculated for foils placed between pellets of the control rod and at the rod surface. Results for foils at the rod surface were difficult to interpret. Measurements in the rod interior showed trends similar to those observed for boron capture. The C/E ratio for fission was consistent within each pin but

was 2% to 3% higher in the interior pin³ than in the other two pins. The consistent C/E within the pins means that the calculated axial reaction rate profiles agree well with the measurements. While there are not enough data from ZPPR-12MB to be conclusive, it appears that ^{235}U measurements are potentially useful for testing the calculated ^{10}B reaction rate profiles in a control rod.

In addition to comparisons of measured and calculated reaction rate profiles, two other C/E comparisons are of interest. One is the boron capture in the rod relative to the fission in the core regions. This is of interest because it allows estimates to be made of control rod reaction rates from the power in the fuel regions. The second comparison is the boron capture to uranium fission in the spectrum of the control rod. This second comparison is of interest in comparing the HAFM and foil techniques for their ability to verify calculated reaction rates in the control rod. In ZPPR-12MB, the average C/E value for boron capture in the rod to fission in the core was 0.945 ± 0.012 while the average C/E for capture in the rod to fission in the rod (omitting fission values at the rod surface) was 0.914 ± 0.022 . Previous measurements⁷ using the HAFM technique in the core region of ZPPR-13 gave a C/E for the boron capture to uranium fission ratio of 0.921 ± 0.012 . These C/E ratios for boron capture to uranium fission are consistent with previous work by Farrar and Oliver⁵⁻⁶ in experiments in other benchmark fast neutron spectra. The difference in C/E ratio from unity is attributed to inaccuracies in the ENDF cross sections for boron capture above about 0.1 MeV.

Conclusions

The measurements in ZPPR-12MB indicate that the HAFM technique can provide useful, direct measurements of the $^{10}\text{B}(n,\text{He})$ reaction rates within a control rod. Boron capture rates were underestimated by calculations by about 8% in the spectrum of the control rod. This underestimation using ENDF-B/IV cross sections is consistent with results from other fast neutron spectra. A future experiment in a larger, more prototypic control rod assembly is planned.

REFERENCES

1. J.L. Rowlands, et al., "The Development and Validation of Control-Rod Calculation Methods," Int. Symp. on Fast Reactor Physics, Aix-en-Provence, France, 24-28 September, 1979, IAEA-XM-244/36, p. 83, IAEA (1980).
2. H.F. McFarlane and P.J. Collins, "Control Rods in LMFBRs: A Physics Assessment," ANL-82-13, Argonne National Laboratory (1982).
3. A.M. Broomfield, et al., "The Mozart Control Rod Experiments and Their Interpretation," Proc. of the International Symp. on Physics of Fast Reactors, Tokyo, October 16-19, 1973, Vol. I. p. 312.
4. H. Farrar IV, et al., "Helium Production Cross Section of Boron for Fast-Reactor Neutron Spectra," Nuclear Technology, 25, p. 305 (1975).
5. H. Farrar IV, et al., "Helium Generation Reaction Rates for ^6Li and ^{10}B in Benchmark Facilities," Proc. of the 3rd ASTM-EURATOM Symp. on Reactor Dosimetry, EUR 6813 EN-FR. Vol. 1, p. 552 (1980).
6. B.M. Oliver, et al., "Spectrum-Integrated Helium Generation Cross Sections for ^6Li and ^{10}B in the Sigma Sigma and Fission Cavity Standard Neutron Fields," Proc. of the 4th ASTM-EURATOM Symp. of Reactor Dosimetry, NUREG/CP-0029, Vol. 2, pp. 889-901 (1982).
7. B.M. Oliver, et al., "Measurements of the ^{10}B Reaction Rate in ZPPR," Presented to the International Conference on Nuclear Data for Basic and Applied Sciences, May 13-17, 1985, Santa Fe, New Mexico.
8. B.M. Oliver, et al., "Helium Concentration in the Earth's Lower Atmosphere," Geochimica et Cosmochimica Acta, 48, p. 1759 (1984).
9. D.W. Maddison, "Computer-Controlled Four-Detector Gamma-Ray Counting System," in Computers in Activation Analysis and Gamma-Ray Spectroscopy, DOE Symp. Series 49, p. 708 (1979).
10. D.W. Maddison, "Development of a Program for Reduction of Large Numbers of Gamma-Ray Spectra," op cit p. 230 (1979).
11. S.B. Brumbach and D. W. Maddison, "Reaction Rate Calibration Techniques at ZPPR for ^{239}Pu Fission, ^{235}U Fission, ^{238}U Fission, and ^{238}U Capture," ANL-82-38, Argonne National Laboratory (1982).
12. R.D. McKnight et al., "Validation Studies of ENDF/MC²-2/SDX Cell Homogenization Path," Proc. of the Topical Meeting on Advances in Reactor Physics and Core Thermal Hydraulics, NUREG/CR-0034, Vol. 1, p. 406 (1982).
13. R. D. Lawrence, "Three-Dimensional Nodal Diffusion and Transport Methods for the Analysis of Fast-Reactor Critical Experiments," Trans. Topical Meeting Reactor Physics and Shielding, Chicago, Illinois, September 17-19, 1984, pp. 814-828 (1984).

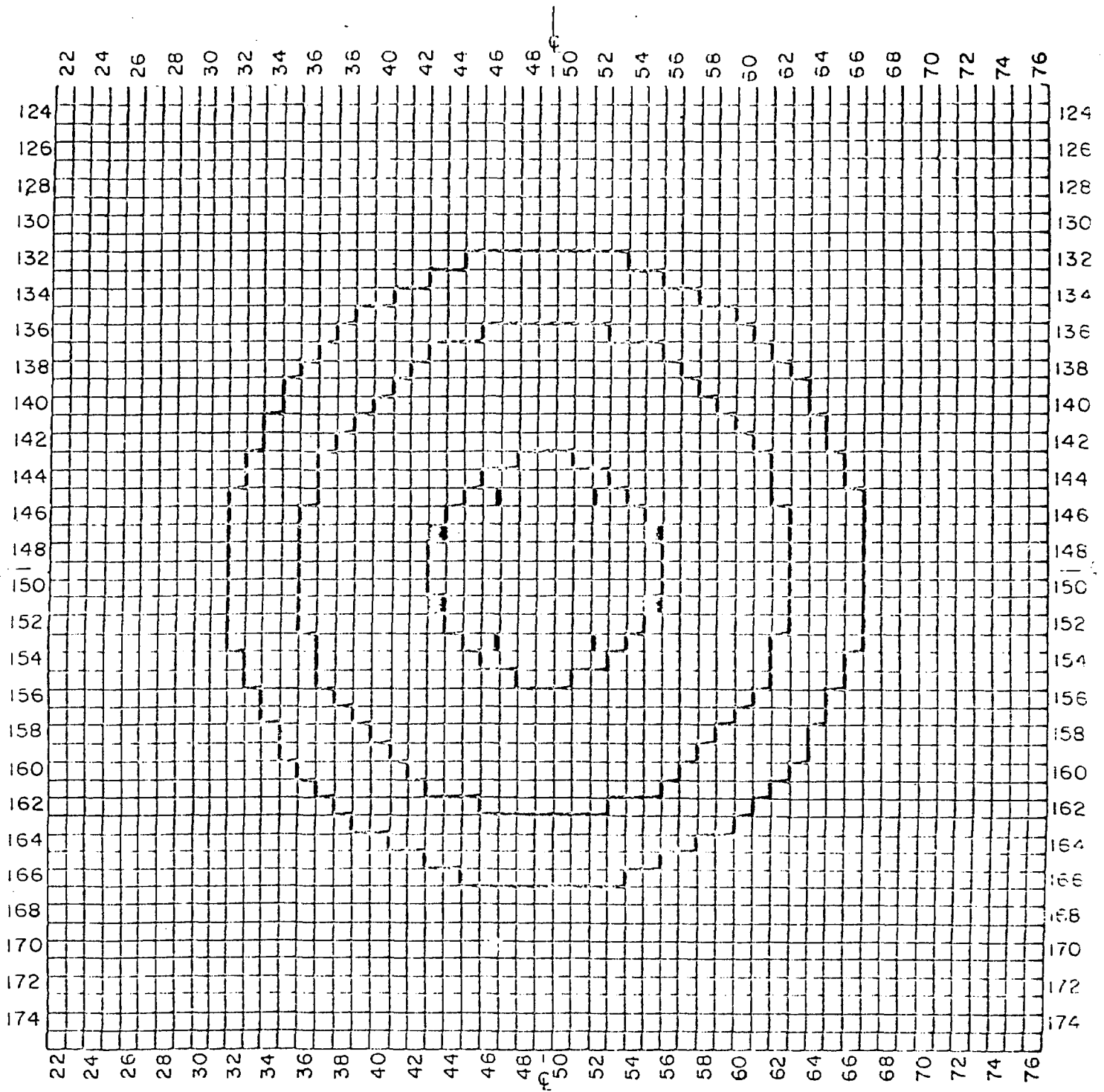


Fig. 1. Core Outline for the ZPPR-12 Metal Blanket Core.

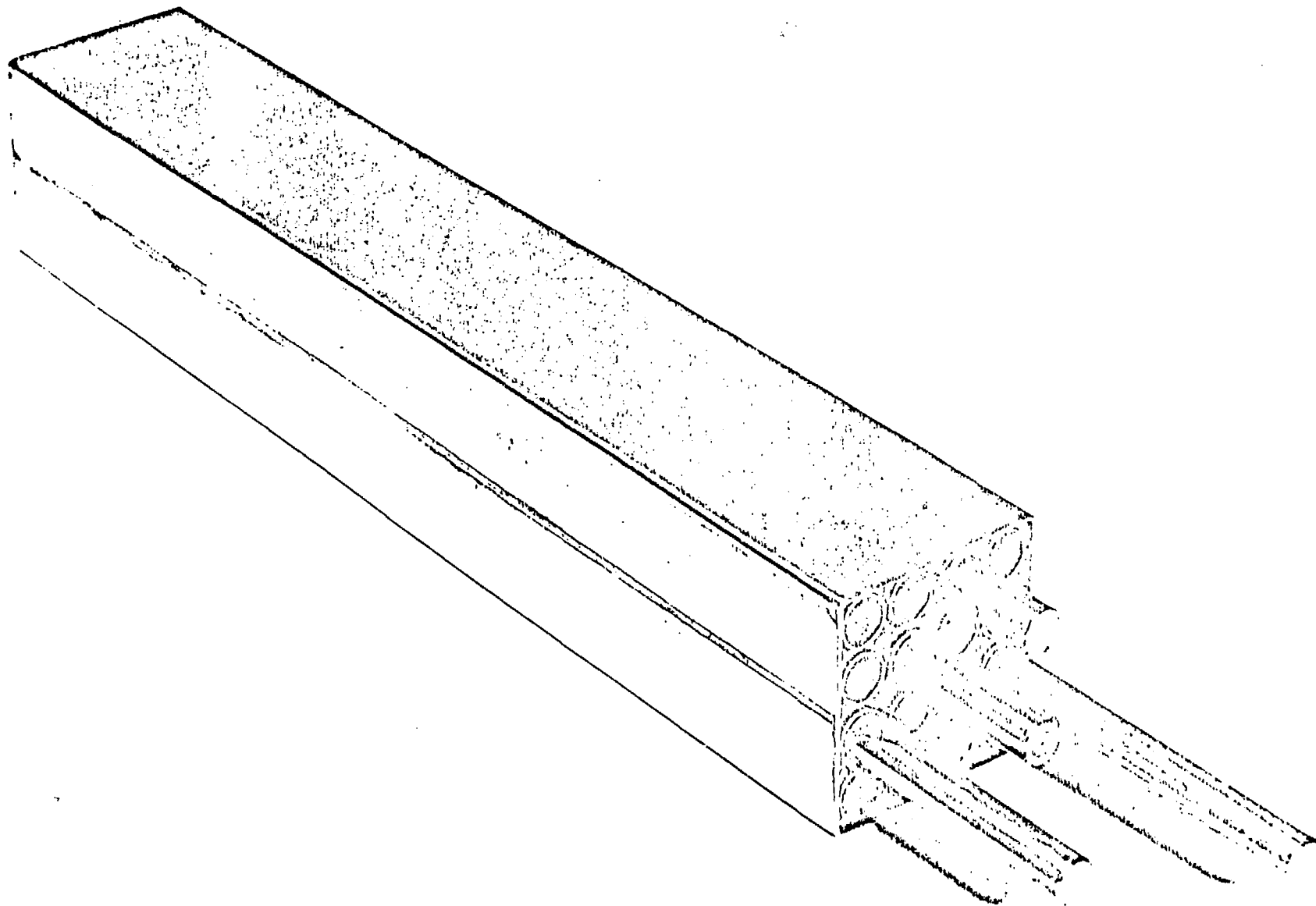


Fig. 2. Calandria Containing Stainless Steel Pins.

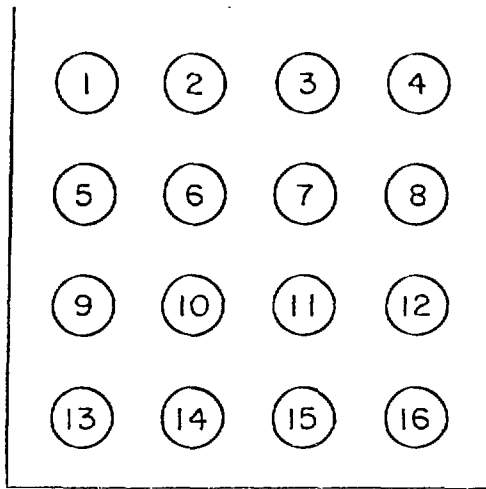


Fig. 3. Numbering scheme for pins in calandria.

0.787			
0.938			
0.768	0.788		
0.960	0.954		
0.826			
0.938			

Z = 69.8 mm

0.838			
0.938			
0.818	0.788		
0.961	0.954		
0.895			
0.921			

Z = 31.8 mm

0.942			
0.944			
0.935	0.901		
0.951	0.938		
1.000			
0.939			

Z = 6.4 mm

xxxx	x = Measured
yyyy	Relative Rate

y = C/E

Fig. 4. Measured Values and C/E Values for $^{10}\text{B}(n,\text{He})$ in ZPPR-12MB.

TABLE 1. Measured Helium Production Rates and Calculation Comparisons in ZPPR-12MB

Pin Number	Pin Type	Isotope	Distance from Rod Tip, mm	Measured Reaction Rate ^a	C/E
13	Corner	¹⁰ B	0-12.7	5.834	0.939
13	Corner	¹⁰ B	25.4-38.1	5.219	0.921
13	Corner	¹⁰ B	63.5-76.2	4.816	0.938
9 ^b	Edge	¹⁰ B	6.4	5.455	0.951
9 ^b	Edge	¹⁰ B	31.8	4.771	0.961
9 ^b	Edge	¹⁰ B	69.8	4.481	0.960
5	Edge	¹⁰ B	0-12.7	5.497	0.944
5	Edge	¹⁰ B	25.4-38.1	4.887	0.938
5	Edge	¹⁰ B	63.5-76.2	4.590	0.938
10	Interior	¹⁰ B	0-12.7	5.257	0.938
10	Interior	¹⁰ B	25.4-38.1	4.598	0.954
10	Interior	¹⁰ B	63.5-76.2	4.211	0.977
4	Corner	⁶ Li	0-12.7	3.380	0.951
4	Corner	⁶ Li	25.4-38.1	3.081	0.952
4	Corner	⁶ Li	63.5-76.2	2.949	0.937
8	Edge	⁶ Li	0-12.7	3.059	1.015
8	Edge	⁶ Li	25.4-38.1	2.897	0.982

^aUnits of 10^{-17} reactions per atom per second at a reactor power of approximately 1 watt.

^bRadially oriented HAFM. All other HAFMs were oriented axially.

TABLE 2. Measured Fission Rates in the ZPPR-12MB
Control Rod

<u>Pin Number</u>	<u>Pin Type</u>	<u>Distance from Rod Tip, mm</u>	<u>Measured Fission Rate^a</u>	<u>C/E</u>
16	Corner	0	5.632	0.977
16	Corner	25.4	4.809	1.014
16	Corner	50.8	4.610	1.009
16	Corner	76.2	4.483	0.999
12	Edge	0	5.517	0.959
12	Edge	25.4	4.638	1.018
12	Edge	50.8	4.413	1.020
12	Edge	76.2	4.253	1.019
11	Interior	0	5.393	0.946
11	Interior	25.4	4.360	1.049
11	Interior	50.8	4.147	1.052
11	Interior	76.2	4.032	1.041

^aUnits of 10^{-17} fissions per atom per second at a reactor power of approximately 1 watt.

TABLE 3. Measured $^{235}\text{U}(n,f)$ Rates and C/E
Values in the Fuel Region of ZPPR-12MB

Positive x-axis			Negative x-axis		
Matrix Location	E ^a	C/E	Matrix Location	E ^a	C/E
149-50	5.637	0.986	149-48	5.604	0.992
149-51	6.098	0.998	149-47	6.092	0.999
149-52	5.923	0.998	149-46	5.878	1.006
149-53	5.438	1.000	149-45	5.401	1.007
149-54	4.735	1.003	149-44	4.711	1.008
149-55	3.853	1.011	148-43	3.793	1.007
Positive y-axis			Negative y-axis		
148-49	5.804	0.998	150-49	5.757	0.996
147-49	6.095	0.997	151-49	6.047	1.005

^aUnits of 10^{-17} fissions per atom per second at a reactor power of approximately 1 watt.

TABLE 4.

Measured and Calculated Relative Boron Capture
Rates within Pins in ZPPR-12MB

Distance from Rod Tip, mm	Corner Pin (13)		Edge Pin (9) ^a		Edge Pin (5)		Interior Pin (10)	
	Measured	Calculated	Measured	Calculated	Measured	Calculated	Measured	Calculated
0-12.7	1.000	1.000	1.000	1.000	1.000	1.000	1.000	1.000
25.4-33.1	0.895	0.878	0.875	0.884	0.889	0.884	0.875	0.859
63.5-76.2	0.826	0.825	0.821	0.830	0.835	0.830	0.801	0.834

^aRadially oriented HAFM. All other HAFMs axially oriented.

TABLE 5. Measured and Calculated Relative Fission Rates
within Pins in ZPPR-12MB

<u>Distance from Rod Tip, mm</u>	<u>Corner Pin (16)</u>		<u>Edge Pin (12)</u>		<u>Interior Pin (11)</u>	
	<u>Measured</u>	<u>Calculated</u>	<u>Measured</u>	<u>Calculated</u>	<u>Measured</u>	<u>Calculated</u>
25.4	1.000	1.000	1.000	1.000	1.000	1.000
50.8	0.959	0.954	0.952	0.954	0.951	0.953
76.2	0.932	0.918	0.917	0.918	0.925	0.918